Numerical Calculation of the Electrorotation Velocity of Latex-Type Particles

Viviana Zimmerman,*,† Vladimir N. Shilov,‡ José Juan López-García,§ and Constantino Grosse†,||

Departamento de Física, Universidad Nacional de Tucumán, Av. Independencia 1800, (4000) S.M. de Tucumán, Argentina, Institute of Biocolloid Chemistry, Ukrainian Academy of Sciences, Kiev, Ukraine, Departamento de Física, Facultad de Ciencias Experimentales, Universidad de Jaén, Campus de las Lagunillas s/n. 23071 Jaén, Spain, and Consejo Nacional de Investigaciones Científicas y Técnicas, Argentina

Received: May 16, 2002; In Final Form: October 15, 2002

The electrorotation velocity of spherical colloidal polystyrene particles suspended in an electrolyte solution is numerically calculated using a network simulation method. The expression for the electroosmotic contribution to the electrorotation used in previous works is generalized for the case of thick double layers. The results are in good agreement with the existing theoretical results when applicable, and they extend to ranges where these theories cannot be applied.

1. Introduction

The dielectric and electrokinetic properties of colloidal particle suspensions have been widely studied using different techniques such as dielectric spectroscopy, electrophoresis, electrorotation, and dielectrophoresis. The importance of these various approaches to basically the same systems lies on some discrepancies encountered between the results obtained using the different techniques. As an example, parameters such as the surface conductivity determined from low-frequency dielectric spectroscopy measurements, do not coincide with those obtained from electrophoresis experiments. Hence, the use of different techniques leads both to complementary understanding of the systems and to their own improvement. Although all the mentioned techniques have been studied using theoretical[1−4] and experimental methods,[5−10] numerical methods were applied only to dielectric spectroscopy[11,12] and electrophoresis.[13,14]

Electrorotation has gained considerable importance in recent years due to the development of microfabrication methodologies used to produce miniaturized sensing devices capable of manipulating and analyzing individual particles as for example cells. Consequently, a full theoretical knowledge of the phenomenon is important, and many works were produced in order to improve its understanding.[4,6−8,15−24] However, most of the theoretical developments lead to expressions only valid under certain conditions, limiting the cases when they can be applied. In this way, a numerical solution is desirable since it might expand the range of cases that can be solved.

In the present work, the electrorotation velocity is for the first time, to our knowledge, calculated using a numerical method. The method used is based on a network simulation method which has been successfully applied over the past few years to study different aspects of the dielectric and electrokinetic properties of colloid systems[12,25,26] and membranes.[27] The procedure consists of discretizating the domain and the differential equations, as in the lineal finite difference method, and establishing the similitude between the discretizated equations in every differential region and the equations that represent an elementary electric circuit composed of basic electronic components (resistors, capacitors, and current and voltage sources). Hence, the solution of the original problem is reduced to the solution of potentials and currents in a network composed of a set of these elementary subcircuits. The direct solution of the governing differential equations is thus avoided, and any commercially available circuit analysis software can be employed to obtain the dynamic behavior of the system.

The system considered for this paper is a polystyrene particle suspended in an electrolyte solution, and it is modeled as usual by a nonconducting charged homogeneous sphere surrounded by a conducting external medium. The results are in good agreement with the existing theoretical results when applicable, and they extend to ranges were these theories cannot be applied.

2. Electrorotation Velocity

The electrorotation velocity is obtained integrating the Navier−Stokes equation with a rotating electric field applied to the system:

$$\eta\nabla^2\vec{v}(\vec{r},t) - \nabla p(\vec{r},t) = e\,(z^+C^+(\vec{r},t) + z^-C^-(\vec{r},t))\,\nabla\phi(\vec{r},t) + \rho_m\left[\frac{\partial\vec{v}(\vec{r},t)}{\partial t} + (\vec{v}(\vec{r},t)\cdot\nabla)\vec{v}(\vec{r},t)\right] \quad (1)$$

where $\vec{v}(\vec{r},t)$ is the velocity of the electrolyte solution, $p(\vec{r},t)$ is the pressure, $\phi(\vec{r},t)$ the electric potential, $z^{\pm}$ and $C^{\pm}(\vec{r},t)$ are the signed valences and number concentrations of positive and negative ions, η and ρ_m the viscosity and mass density of the electrolyte solution, and e is the elementary charge. The rotating field is obtained superposing two perpendicular 90° out-of-phase

* Corresponding author. E-mail: vzimmerman@herrera.unt.edu.ar
† Universidad Nacional de Tucumán.
‡ Ukrainian Academy of Sciences.
§ Universidad de Jaén.
|| Consejo Nacional de Investigaciones Científicas y Técnicas.

10.1021/jp026127n CCC: $22.00
Published on Web 11/23/2002

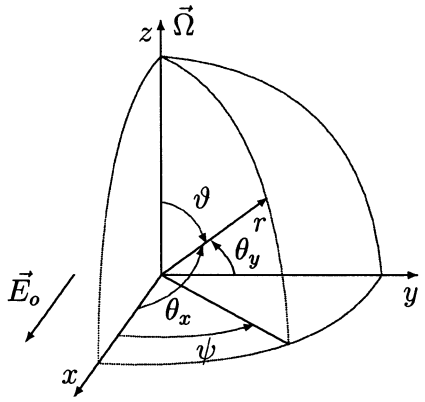

Figure 1. Coordinate system fixed in the laboratory frame, with polar axis coincident with the angular velocity vector. The rotating field is obtained applying two 90° out-of-phase AC electric fields, one pointing in the *x*-direction, and the other one in the *y*-direction. θ_x and θ_y are the polar angles with respect to these fields. The time is set at an instant when the applied electric field points in the *x*-direction.

AC electric fields, and the induced electric potential and ion concentration distributions are assumed as being the superposition of those produced by each of the alternating fields. This hypothesis implies that the particle rotation speed is small compared to the field frequency, which is usually fulfilled in electrorotation experiments.

The calculations are worked out referring the angles to a coordinate system (r, ϑ,ψ) fixed in the laboratory frame, with polar axis coincident with the angular velocity vector (Figure 1). The time is set at an instant when the applied field points in the direction of the *x*-axis (still, the results are general since the angles do not depend on t). In this system, only the ψ component of the fluid velocity contributes to the particle rotation and, consequently, only this component of the Navier−Stokes equation must be integrated. The equation is further simplified considering small Reynolds numbers and taking into account that the problem is stationary and that terms with vanishing curl cannot contribute to the rotation. Then the Navier−Stokes equation reduces to

$$\eta\nabla^2\vec{v}(\vec{r})|_\psi = -\vec{f}^{\,\psi}_{\text{elec}}(\vec{r}) \tag{2}$$

where $\vec{f}^{\,\psi}_{\text{elec}}(\vec{r})$ is the ψ component of the electric force density:

$$\vec{f}^{\,\psi}_{\text{elec}}(\vec{r}) = -e(z^+C^+(\vec{r}) + z^-C^-(\vec{r}))\nabla_\psi\phi(\vec{r}) \tag{3}$$

The only term of the series expansion of the angular distribution of the velocity that contributes to the particle rotation is given by sin ϑ. Since this same angular dependence also determines the long-range asymptotic behavior of the fluid velocity with respect to the rotating particle, the only term that needs to be considered is

$$\vec{v}(\vec{r}) = \vec{v}(r)\sin\vartheta \tag{4}$$

so, the first term of equation 2 reduces to

$$\eta\nabla^2\vec{v}(\vec{r})|_\psi = \eta\left(\frac{\mathrm{d}^2v_\psi(r)}{\mathrm{d}r^2} + \frac{2}{r}\frac{\mathrm{d}v_\psi(r)}{\mathrm{d}r} - \frac{2}{r^2}v_\psi(r)\right)\sin\vartheta\,\hat{e}_\psi \tag{5}$$

The ion concentrations and electric potential distributions that appear in the expression for the electric force density (eq 3) can be expressed in terms of their equilibrium values, which depend only on the distance to the particle due to the spherical symmetry of the problem:

$$\phi(\vec{r}, t) = \phi_o(r) + \delta\phi(\vec{r}, t) \tag{6}$$

$$C^\pm(\vec{r}, t) = C^\pm_o(r) + \delta C^\pm(\vec{r}, t) \tag{7}$$

where $\delta C^\pm(\vec{r}, t)$ and $\delta\phi(\vec{r}, t)$ are the field induced changes of the ion concentrations and electric potential distributions. Hence, keeping only terms that can contribute to the rotation, the electric force density reduces to

$$\vec{f}^{\,\psi}_{\text{elec}}(\vec{r}) = -e(z^+\delta C^+(\vec{r}) + z^-\delta C^-(\vec{r}))\nabla_\psi\delta\phi(\vec{r}) \tag{8}$$

As previously noted, the electric potential and ion concentration distributions are the superposition of distributions generated by two perpendicular 90° out-of-phase AC electric fields. Due to their difference in phase, these distributions can be expressed as

$$\delta C^\pm_x(\vec{r}) = \mathrm{Re}\{\delta C^\pm(r)\}\cos\theta_x = \mathrm{Re}\{\delta C^\pm(r)\}\sin\vartheta\cos\psi \tag{9}$$

$$\delta C^\pm_y(\vec{r}) = \mathrm{Im}\{\delta C^\pm(r)\}\cos\theta_y = \mathrm{Im}\{\delta C^\pm(r)\}\sin\vartheta\sin\psi \tag{10}$$

$$[\nabla_\psi\delta\phi(\vec{r})]_x = \mathrm{Re}\{\nabla_\psi[\delta\phi(r)\cos\theta_x]\} = -\mathrm{Re}\left\{\frac{\delta\phi(r)}{r}\right\}\sin\psi\,\hat{e}_\psi \tag{11}$$

$$[\nabla_\psi\delta\phi(\vec{r})]_y = \mathrm{Im}\{\nabla_\psi[\delta\phi(r)\cos\theta_y]\} = \mathrm{Im}\left\{\frac{\delta\phi(r)}{r}\right\}\cos\psi\,\hat{e}_\psi \tag{12}$$

where θ_x and θ_y are the polar angles referred to the symmetry axes of the two distributions (*x* and *y* in Figure 1). Replacing these expressions in equation 8 and taking into account that the terms in (sin ψ cos ψ) cannot contribute to the rotation, the electric force density results

$$f^\psi_{\text{elec}}(\vec{r}) = \frac{-e}{r}[\mathrm{Re}\{z^+\delta C^+(r) + z^-\delta C^-(r)\}\mathrm{Im}\{\delta\phi(r)\}\cos^2\psi - \mathrm{Im}\{z^+\delta C^+(r) + z^-\delta C^-(r)\}\mathrm{Re}\{\delta\phi(r)\}\sin^2\psi]\sin\vartheta \tag{13}$$

Finally, replacing 5 and 13 in 2, and averaging over ψ, leads to the following differential equation for the tangential velocity:

$$\frac{\mathrm{d}^2v_\psi(r)}{\mathrm{d}r^2} + \frac{2}{r}\frac{\mathrm{d}v_\psi(r)}{\mathrm{d}r} - \frac{2}{r^2}v_\psi(r) = \frac{g(r)}{\eta} \tag{14}$$

where

$$g(r) = \frac{e}{2r}[\mathrm{Re}\{z^+\delta C^+(r) + z^-\delta C^-(r)\}\mathrm{Im}\{\delta\phi(r)\} - \mathrm{Im}\{z^+\delta C^+(r) + z^-\delta C^-(r)\}\mathrm{Re}\{\delta\phi(r)\}] \tag{15}$$

This equation can be expressed in terms of the angular rotation speed

$$\Omega(r) = \frac{v_\psi(r)}{r} \tag{16}$$

and analytically integrated, leading to

$$\Omega(r) = C_1 + \frac{C_2}{r^3} + \frac{1}{3\eta}\int_a^r g(x)\,\mathrm{d}x - \frac{1}{3\eta r^3}\int_a^r x^3 g(x)\,dx \quad (17)$$

where a is the particle radius, and C_1 and C_2 are integration constants. Their values are obtained using the following boundary conditions:

- the angular velocity must vanish far from the particle,

$$\Omega(r\rightarrow\infty) = C_1 + \frac{1}{3\eta}\int_a^\infty g(x)\,\mathrm{d}x = 0$$

and consequently,

$$C_1 = -\frac{1}{3\eta}\int_a^\infty g(x)\,dx \quad (18)$$

- at steady-state conditions, the total torque acting on any spherical volume concentric with the particle must be zero,

$$\vec{T}(r) = \vec{T}_{\text{viscous}}(r) + \vec{T}_{\text{electric}}(r) = 0 \quad (19)$$

The viscous torque is calculated integrating the viscous stress tensor on a spherical surface of radius r:

$$\begin{aligned}\vec{T}_{\text{viscous}}(r) &= \int_S \vec{r}\times(\sigma_{\text{rr}}\hat{e}_{\text{r}} + \sigma_{\vartheta\text{r}}\hat{e}_\vartheta + \sigma_{\psi\text{r}}\hat{e}_\psi)\,\mathrm{ds} = \\ &= \int_S(\sigma_{\vartheta\text{r}}\hat{e}_\psi - \sigma_{\psi\text{r}}\hat{e}_\vartheta)r\,\mathrm{ds} = \int_S \sigma_{\psi\text{r}} r\sin\vartheta\,ds\,\hat{k} = \\ &= \int_S\left[\frac{\partial}{\partial r}(v_\psi(r)\sin\vartheta) - \frac{v_\psi(r)\sin\vartheta}{r}\right]r^3\sin^2\vartheta\,\mathrm{d}\vartheta\,\mathrm{d}\psi\,\hat{k} = \\ &= \frac{8\pi}{3}\eta r^3\left(\frac{\mathrm{d}v_\psi(r)}{\mathrm{d}r} - \frac{v_\psi(r)}{r}\right)\hat{k} \\ &= \frac{8\pi}{3}\eta r^4\left(\frac{\mathrm{d}\Omega(r)}{\mathrm{d}r}\right)\hat{k} \end{aligned} \quad (20)$$

where $\hat{e}_{\text{r}}$, $\hat{e}_\vartheta$, $\hat{e}_\psi$ are the unit vectors corresponding to the spherical coordinate system shown in Figure 1, and $\hat{k}$ is the unit vector in the direction of the polar axis in the same figure.

The electric torque is

$$\begin{aligned}\vec{T}_{\text{electric}}(r) &= \int_{V_{\text{int}}}\vec{r}\times\vec{f}_{\text{elec}}(\vec{r})\,\mathrm{d}V \\ &= \vec{T}_{\text{electric}}(r\rightarrow\infty) - \int_{V_{\text{ext}}}\vec{r}\times\vec{f}_{\text{elec}}(\vec{r})\,\mathrm{d}V \end{aligned} \quad (21)$$

where V_{int} is a spherical volume of radius r and V_{ext} is all the volume outside it, used in order to avoid the calculation of the torque inside the particle. $\vec{T}_{\text{electric}}(r\rightarrow\infty)$ represents the integral over the whole space and can be easily calculated as the product of the dipole moment ($\vec{d}$) and the applied electric field ($\vec{E}_o$):

$$\begin{aligned}\vec{T}_{\text{electric}}(r\rightarrow\infty) &= \vec{d}\times\vec{E}_o \\ &= -4\pi\epsilon_o\epsilon E_o\lim_{r\rightarrow\infty}[r^2\,\mathrm{Im}\{\delta\phi(r) + E_o r\}]\hat{k} \end{aligned} \quad (22)$$

while the integral is

$$\begin{aligned}\int_{V_{\text{ext}}}\vec{r}\times\vec{f}_{\text{elec}}(\vec{r})\,\mathrm{d}V &= \int_{V_{\text{ext}}} r f^{\psi}_{\text{elec}}(\vec{r})\sin\vartheta\,\mathrm{d}V\,\hat{k} \\ &= -\frac{8\pi}{3}\int_r^\infty x^3 g(x)\,\mathrm{d}x\,\hat{k} \end{aligned} \quad (23)$$

Therefore, the electric torque reduces to

$$\begin{aligned}\vec{T}_{\text{electric}}(r) = &-4\pi\epsilon_o\epsilon E_o\lim_{r\rightarrow\infty}[r^2\,\mathrm{Im}\{\delta\phi(r) + E_o r\}]\hat{k} + \\ &\frac{8\pi}{3}\int_r^\infty x^3 g(x)\,\mathrm{d}x\,\hat{k} \end{aligned} \quad (24)$$

where ϵ is the relative permittivity of the electrolyte solution, and ϵ_o is the permittivity of free space. In classical electrorotation theory, the electric torque is usually expressed in terms of the imaginary part of the Clausius Mossotti factor[6,15,17] (Im U^*) that in terms of the notation used in the present paper is

$$\mathrm{Im}\{U^*\} = \frac{1}{a^3 E_o}\lim_{r\rightarrow\infty}[r^2\,\mathrm{Im}\{\delta\phi(r) + E_o r\}]$$

Replacing the expressions for the viscous and electric torques (eqs 20 and 24) in equation 19 leads to

$$C_2 = \frac{1}{3\eta}\int_a^\infty x^3 g(x)\,\mathrm{d}x - \frac{\epsilon_o\epsilon E_o}{2\eta}\lim_{r\rightarrow\infty}[r^2\,\mathrm{Im}\{\delta\phi(r) + E_o r\}] \quad (25)$$

Finally, the angular rotation speed of the liquid is obtained substituting the constants C_1 and C_2 in eq 17,

$$\begin{aligned}\Omega(r) = &-\frac{1}{3\eta}\int_r^\infty g(x)\,\mathrm{d}x + \frac{1}{3\eta r^3}\int_r^\infty x^3 g(x)\,\mathrm{d}x - \\ &\frac{\epsilon_o\epsilon E_o}{2\eta r^3}\lim_{r\rightarrow\infty}[r^2\,\mathrm{Im}\{\delta\phi(r) + E_o r\}] \end{aligned} \quad (26)$$

Considering the adherence condition of the liquid on the particle surface, the angular rotation speed of the particle results

$$\begin{aligned}\Omega_{\text{particle}} = \Omega(a) = &-\frac{\epsilon_o\epsilon E_o}{2\eta a^3}\lim_{r\rightarrow\infty}[r^2\,\mathrm{Im}\{\delta\phi(r) + E_o r\}] - \\ &\frac{1}{3\eta}\int_a^\infty\left(1 - \frac{x^3}{a^3}\right)g(x)\,\mathrm{d}x \end{aligned} \quad (27)$$

The first term in the right-hand side of this equation represents the classical expression for the electrorotation speed of a spherical particle, while the second one represents the electroosmotic contribution to electrorotation calculated without the thin double layer approximation used in previous works.[4,22−24]

In all existing calculations related to electrorotation, the first term (proportional to the induced dipole moment) was always determined analytically. In the present work this term, as well as the function $g(x)$ and its integral, are all calculated numerically.

3. Electric Potential and Ion Concentrations

To obtain the induced dipole moment and the function $g(x)$ appearing in eq 27, the electric potential ($\phi(\vec{r}, t)$), the ion number concentrations ($C^{\pm}(\vec{r}, t)$), and the velocity of the electrolyte

solution ($\vec{v}(\vec{r}, t)$) must be calculated solving the following system of equations:

• Poisson equation:

$$\nabla^2\phi(\vec{r}, t) = -\frac{e}{\epsilon_o \epsilon}(z^+C^+(\vec{r}, t) + z^-C^-(\vec{r}, t)) \quad (28)$$

• Nernst−Planck equations:

$$\vec{j}^{\pm}(\vec{r}, t) = -D^{\pm}\nabla C^{\pm}(\vec{r}, t) - \frac{ez^{\pm}D^{\pm}}{kT}C^{\pm}(\vec{r}, t)\nabla\phi(\vec{r}, t) + C^{\pm}(\vec{r}, t)\vec{v}(\vec{r}, t) \quad (29)$$

• Continuity equations: $\nabla\cdot\vec{j}^{\pm}(\vec{r}, t) = -\frac{\partial C^{\pm}(\vec{r}, t)}{\partial t}$ (30)

• Navier−Stokes equation (eq 1)

• Condition of incompressible fluid: $\nabla\cdot\vec{v}(\vec{r}, t) = 0$ (31)

where $D^{\pm}$ and $\vec{j}^{\pm}(\vec{r}, t)$ are the diffusion coefficients and fluxes of positive and negative ions, k is the Boltzmann constant, and T the temperature.

To separate the equilibrium from the nonequilibrium parts of the equation system, the electric potential and ion concentrations are expressed in terms of their equilibrium values (eqs 6 and 7). Then, for weak fields, and keeping only linear terms in the field, the system reduces to

equilibrium equations:

$$\nabla^2\tilde{\phi}_o(r) = \frac{-e^2}{\epsilon_o \epsilon kT}(z^+C_o^+(r) + z^-Co^-(r)) \quad (32)$$

$$C_o^{\pm}(r) = c_{\infty}^{\pm}\exp(-z^{\pm}\tilde{\phi}_o(r)) \quad (33)$$

nonequilibrium equations:

$$\nabla^2\delta\tilde{\phi}(\vec{r}, t) = \frac{-e^2}{\epsilon_o \epsilon kT}[z^+Co^+(r)\delta\tilde{\mu}^+(\vec{r}, t) + z^-Co^-(r)\delta\tilde{\mu}^-(\vec{r}, t) - ((z^+)^2C_o^+(r) + (z^-)^2C_o^-(r))\delta\tilde{\phi}(\vec{r}, t)] \quad (34)$$

$$\nabla^2\delta\tilde{\mu}^{\pm}(\vec{r}, t) = \frac{1}{D^{\pm}}\frac{\partial}{\partial t}(\delta\tilde{\mu}^{\pm}(\vec{r}, t) - z^{\pm}\delta\tilde{\phi}(\vec{r}, t)) + z^{\pm}\nabla\tilde{\phi}_o(r)\cdot\left(\nabla\delta\tilde{\mu}^{\pm}(\vec{r}, t) - \frac{1}{D^{\pm}}\vec{v}(\vec{r}, t)\right) \quad (35)$$

$$\eta\nabla^2\vec{b}(\vec{r}, t) = -kT\nabla\tilde{\phi}_o(r) \times [z^+C_o^+(r)\nabla\delta\tilde{\mu}^+(\vec{r}, t) + z^-Co^-(r)\nabla\delta\tilde{\mu}^-(\vec{r}, t)] + \rho_m\frac{\partial\vec{b}(\vec{r}, t)}{\partial t} \quad (36)$$

where $\delta\tilde{\mu}^{\pm}(\vec{r}, t)$ are the dimensionless electrochemical potentials, introduced in order to simplify the forthcoming calculations,

$$\delta\tilde{\mu}^{\pm}(\vec{r}, t) = \frac{\delta C^{\pm}(\vec{r}, t)}{C_o^{\pm}(r)} + z^{\pm}\delta\tilde{\phi}(\vec{r}, t) \quad (37)$$

$c_{\infty}^{\pm}$ are the equilibrium number concentration of positive and negative ions very far from the particle, and $\vec{b}(\vec{r}, t)$ is the vorticity

$$\vec{b}(\vec{r}, t) = \text{curl}\ \vec{v}(\vec{r}, t) \quad (38)$$

introduced in order to avoid the calculation of the pressure. The mark ~ placed over the potentials stands for their dimensionless forms:

$$\tilde{\phi}(\vec{r}, t) = \frac{e}{kT}\phi(\vec{r}, t)$$

It must be noted at this point that the potential, ion concentrations, and velocity distributions calculated in this section are of first order in the field. Therefore, the tangential velocity calculated in the previous section is of second order in the field (eq.14) and, consequently, it is independent of the velocity calculated here.

The variables $\delta\tilde{\phi}(\vec{r}, t)$ and $\delta C^{\pm}(\vec{r}, t)$ used so far, have a clear physical meaning. However, numerical problems in the calculation of the function $g(r)$ (eq 15), related to small differences in variables with large absolute values, are overcome using a new set of variables. These variables are obtained considering a virtual system (usually called *thermostat*) which is everywhere neutral and in local equilibrium with the real system.[4] The new variables are defined as follows:

$$\delta\tilde{\mu}^{\pm}(\vec{r}, t) = \frac{\delta c(\vec{r}, t)}{c_{\infty}} + z^{\pm}\tilde{\varphi}(\vec{r}, t) \quad (39)$$

$$\delta\tilde{\phi}(\vec{r}, t) = \tilde{\varphi}(\vec{r}, t) + \tilde{\Phi}(\vec{r}, t) \quad (40)$$

where c_{∞} and $\delta c(\vec{r}, t)$ are the equilibrium and field-induced change of the electrolyte concentration of salt in the thermostat (related to the number concentrations of positive and negative ions in the thermostat by $c_{\infty}^{\pm} + \delta c^{\pm}(\vec{r}, t) = \mp z^{\mp}(c_{\infty} + \delta c(\vec{r}, t))$). The symbol $\tilde{\varphi}(\vec{r}, t)$ represents the dimensionless electric potential in the thermostat, and $\tilde{\Phi}(\vec{r}, t)$ the so-called *quasiequilibrium* dimensionless potential. The quasiequilibrium potential is a short-range function, so it has zero value far from the particle, making the real system and the thermostat identical in that region.

The explicit angular dependence of the variables (potentials, concentration, velocity, and vorticity), is obtained considering that the applied field is uniform,

$$\vec{E}(\vec{r}, t) = E_o(t)(\cos\theta\hat{e}_r - \sin\theta\hat{e}_{\theta}) \quad (41)$$

and furthermore, that it is weak. These hypotheses, implicitly used in every electrorotation theory, are valid if the field is uniform within the region where all the field induced changes occur (region of radius $\sim 2(a + 1/\kappa)$,[29] where κ is the reciprocal of the Debye screening length); and if the field-induced change of the electrolyte concentration of salt is everywhere small: $\delta c \ll c_{\infty}$. This last condition is satisfied if $Eea/kT \ll 1$, or $E \ll 10000$ V/m for micron-size particles.[4]

Thus, in view of the axial symmetry of the problem, the variables take the following form:

$$\tilde{\varphi}(\vec{r}, t) = \tilde{\varphi}(r, t)\cos\theta$$

$$\tilde{\Phi}(\vec{r}, t) = \tilde{\Phi}(r, t)\cos\theta$$

$$\delta c(\vec{r}, t) = \delta c(r, t)\cos\theta$$

$$\vec{v}(\vec{r}, t) = v_r(r, t)\cos\theta\,\hat{e}_r - v_{\theta}(r, t)\sin\theta\,\hat{e}_{\theta}$$

$$\vec{b}(\vec{r}, t) = b(r, t)\sin\theta\,\hat{e}_{\varphi}$$

where the arguments (r, t) in the right-hand side mean that the variables do not depend on the angles, but only on the distance to the particle and on the time.

Replacing the thermostat variables (eqs 39 and 40) and taking into account the angular dependence of the variables and ofthe Laplacian, the equation system (eqs 32−36, 38) transforms into

$$\frac{1}{r^2}\frac{\mathrm{d}}{\mathrm{d}r}\left(r^2\frac{\mathrm{d}\tilde{\phi}o}{\mathrm{d}r}\right)=\frac{-e^2c_\infty}{\epsilon_o\,\epsilon kT}[z^+\exp(-z^+\tilde{\phi}_o)+z^-\exp(-z^-\tilde{\phi}_o)] \quad (42)$$

$$\frac{1}{r^2}\frac{\partial}{\partial r}\left(r^2\frac{\partial\tilde{\varphi}}{\partial r}\right)-\frac{2}{r^2}\tilde{\varphi}=-\frac{\Lambda}{D_{\mathrm{ef}}}\frac{\partial}{\partial t}\left(\frac{\delta c}{c_\infty}\right)-\frac{Q}{D_{\mathrm{ef}}}\frac{\partial\tilde{\Phi}}{\partial t}+\frac{\mathrm{d}\tilde{\phi}_o}{\mathrm{d}r}\left[\frac{\partial}{\partial r}\left(\frac{\delta c}{c_\infty}\right)+(z^++z^-)\frac{\partial\tilde{\varphi}}{\partial r}-\frac{Q}{D_{\mathrm{ef}}}\upsilon_r\right] \quad (43)$$

$$\frac{1}{r^2}\frac{\partial}{\partial r}\left[r^2\frac{\partial}{\partial r}\left(\frac{\delta c}{c_\infty}\right)\right]-\frac{2}{r^2}\frac{\delta c}{c_\infty}=\frac{1}{D_{\mathrm{ef}}}\frac{\partial}{\partial t}\left(\frac{\delta c}{c_\infty}\right)-z^+z^-\frac{\Lambda}{D_{\mathrm{ef}}}\frac{\partial\tilde{\Phi}}{\partial t}-z^+z^-\frac{\mathrm{d}\tilde{\phi}_o}{\mathrm{d}r}\left(\frac{\partial\tilde{\varphi}}{\partial r}+\frac{\Lambda}{D_{\mathrm{ef}}}\upsilon_r\right) \quad (44)$$

$$\frac{1}{r^2}\frac{\partial}{\partial r}\left(r^2\frac{\partial\tilde{\Phi}}{\partial r}\right)-\frac{2}{r^2}\tilde{\Phi}=\frac{\Lambda}{D_{\mathrm{ef}}}\frac{\partial}{\partial t}\left(\frac{\delta c}{c_\infty}\right)+\frac{Q}{D_{\mathrm{ef}}}\frac{\partial\tilde{\Phi}}{\partial t}-\frac{\mathrm{d}\tilde{\phi}_o}{\mathrm{d}r}\left[\frac{\partial}{\partial r}\left(\frac{\delta c}{c_\infty}\right)+(z^++z^-)\frac{\partial\tilde{\varphi}}{\partial r}-\frac{Q}{D_{\mathrm{ef}}}\upsilon_r\right]-\frac{e^2}{\epsilon_o\epsilon kT}\left[(z^+Co^++z^-Co^-)\frac{\delta c}{c_\infty}-[(z^+)^2C_o^++(z^-)^2C_o^-]\tilde{\Phi}\right] \quad (45)$$

$$\frac{\eta}{r^2}\frac{\partial}{\partial r}\left(r^2\frac{\partial b}{\partial r}\right)-\frac{2\eta}{r^2}b=\rho_{\mathrm{m}}\frac{\partial b}{\partial t}+\frac{kT}{r}\frac{\mathrm{d}\tilde{\phi}_o}{\mathrm{d}r}\left[(z^+C_o^++z^-C_o^-)\frac{\delta c}{c_\infty}+[(z^+)^2C_o^++(z^-)^2C_o^-]\tilde{\varphi}\right] \quad (46)$$

$$b=-\frac{r}{2}\frac{\partial^2\upsilon_r}{\partial r^2}-2\frac{\partial\upsilon_r}{\partial r} \quad (47)$$

where

$$\Lambda=\frac{D^+-D^-}{D^+z^+-D^-z^-} \quad (48)$$

$$D_{\mathrm{ef}}=\frac{D^+D^-(z^+-z^-)}{D^+z^+-D^-z^-} \quad (49)$$

$$Q=\frac{z^+D^--z^-D^+}{D^+z^+-D^-z^-} \quad (50)$$

The angular variable θ cancels out in every equation, so the solution of the equation system is valid for any value of θ. Consequently, r and t remain as the only independent variables, but their dependence was omitted in the preceding equations in order to simplify the notation.

3.1. Boundary Conditions. The boundary conditions used for the complete solution of the problem are as follows.[25]

- Equilibrium potential ($\tilde{\phi}o(r)$). It vanishes at infinity and is equal to ζ at $r = a$, since the radius of the particle coincides with the slipping plane in the framework of the standard electrokinetic model.
- Field-induced change of the electric potential ($\delta\tilde{\phi}(r, t)$). At infinity it tends to $-eE_o(t)r/kT$. On the particle surface, the conditions of continuity of the potential and of the normal component of the displacement lead to

$$\delta\tilde{\phi}(a, t)=a\frac{\epsilon}{\epsilon_i}\frac{\partial\delta\tilde{\phi}(r, t)}{\partial r}|_{r=a}$$

where ϵ_i is the relative permittivity of the particle.

- Field-induced change of the electrochemical potentials ($\delta\tilde{\mu}^\pm(r, t)$). According to their definition (eq 37), they tend to $-z^\pm eE_o(t)r/kT$ at infinity, where the field-induced changes of the ion concentrations vanish. On the particle surface, the normal flux of ions and the normal component of the fluid velocity vanish and, since $\vec{J}^\pm(r, t) = \nabla\delta\tilde{\mu}^\pm(r, t) + C^\pm(r, t)\vec{v}(r, t)$,

$$\frac{\partial\delta\tilde{\mu}^\pm(r, t)}{\partial r}|_{r=a}=0$$

- Radial component of the velocity ($\upsilon_r(r, t)$). At infinity it tends to a constant value υ_∞. The non slipping condition on the surface of the impermeable particle together with the incompressibility of the fluid lead to

$$\frac{\partial\upsilon_r(r, t)}{\partial r}|_{r=a}=0$$

- Vorticity ($b(r, t)$). At infinity it is null, and the balance of forces on the surface for a particle with the same mass density as the electrolyte solution leads to:[14,25]

$$b(a, t)-a\frac{\partial b(r, t)}{\partial r}|_a=\frac{kT}{a^2\eta}\int_a^\infty(z^+C_o^+(r)\delta\tilde{\mu}^+(r, t)+z^-C_o^-(r)\delta\tilde{\mu}^-(r, t))\frac{\mathrm{d}\tilde{\phi}_o(r)}{\mathrm{d}r}r^2\,\mathrm{d}r$$

3.2. Numerical Calculations. Since the spatial variable domain is infinite ($a \le r < \infty$), it is convenient to replace the variable r by a dimensionless finite variable which simplifies the discretization of the domain in a finite number of compartments. The new variable should lead to an almost linear variation of the unknown magnitudes. However, as this requirement implies that the solution is known, only approximations or long distance behaviors can be considered. Thus, a spatial variable (ξ_{PB}) with an exponential close range behavior was used for the solution of the equilibrium potential (Poisson−Boltzmann equation, eq 42):

$$\xi_{\mathrm{PB}}=\frac{a}{r}[1+\kappa a\,\mathrm{e}^{-\kappa(r-a)}]$$

where

$$\kappa=\sqrt{\frac{e^2[(z^+)^2c_\infty^++(z^-)^2c_\infty^-]}{\epsilon_o\epsilon kT}}$$

In the case of the non equilibrium problem, the spatial variable used was

$$\xi=\frac{a}{r}$$

and, to obtain linear long distance variations with ξ, the dependent variables were replaced by new dimensionless variables:

$$f(r, t)=\frac{r}{a}\left(\tilde{\varphi}(r, t)+\frac{eE_o}{kT}r\right)$$

$$q(r, t) = \frac{r}{a}\tilde{\Phi}(r, t)$$

$$n(r, t) = \frac{r}{a}\frac{\delta c(r, t)}{c_\infty}$$

$$u(r, t) = \frac{r^2}{aD_{ef}}(v_r(r, t) - v_\infty)$$

$$B(r, t) = \frac{a^2}{D_{ef}}b(r, t)$$

Replacing all these variables in the equation system (eqs 42−47) and the boundary conditions, and after discretization, the network circuits were designed in a way similar to those in references 12 and 25 (see Appendix). For the circuits design, the whole domain was divided into three regions determined by the ζ-potential value and the double layer thickness ($1/\kappa$), and each of these regions was then subdivided into small compartments where the spatial variation of the functions was assumed linear. The width of the compartments ($\Delta\xi$) is constant over every region. The complete network was finally analyzed using the PSPICE package. The input file with the description of the circuit and the output file with the potential values in the circuit were created and interpreted, respectively, using C language programs that are available upon request.

4. Results and Discussion

The numerical results for the ion concentrations and potential distributions are finally used to calculate the electrorotation velocity (eq 27), using a trapezoidal method for the numerical solution of the integral in the second term. Some spectra obtained in this way are shown and compared with theoretical results in Figures 2 to 5. The theoretical data in these figures are the superposition of the rotation spectra related to the α dispersion obtained as in reference 22 and the rotation related to the Maxwell−Wagner dispersion. This last high-frequency data were obtained following the procedure described in reference 24 but replacing the particle used in that work with an insulating particle surrounded by a surface conductivity λ (due to its charge), and modeled as a homogeneous conducting particle with conductivity:

$$\sigma_i = \frac{2\lambda}{a} \tag{51}$$

The electric potential and charge density distributions corresponding to this particle were obtained solving the Poisson, continuity, and Nernst−Planck equations in the external medium, and the Laplace equation inside the particle, with the following boundary conditions: (i) continuity of the electric potential, (ii) continuity of the normal component of the displacement, and (iii) continuity of the normal component of the current density.

A comparison between the numerical and theoretical spectra is presented in Figure 2 for different values of the ζ-potential at a constant κa. The agreement is very good for low values of ζ, but becomes worse for highly charged particles.[29] In Figure 3, the spectra correspond to different values of κa at a constant ζ-potential value. As expected, a good agreement between the theoretical and numerical results is observed only for high values of κa, since the theories used for both the low and the high-frequency regions are valid for thin double layers. When κa is lowered, the differences between the numerical and theoretical results increase, and for $\kappa a \leq 1$ the theories can no longer be used so that only numerical spectra are shown. These last spectra present only a single rotation peak, since the low-frequency peak (related to the α dispersion) is hidden by the Maxwell−Wagner rotation peak.

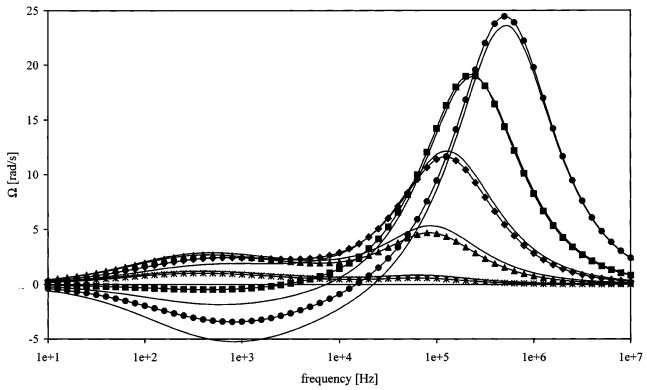

Figure 2. Electrorotation spectra obtained using numerical (lines with symbols) and theoretical (lines) calculations for different values of the ζ-potential: (∗) −50 mV, (▲) −100 mV, (◆) −150 mV, (■) −200 mV, (●) −250 mV. The other parameters are: $a = 2$ μm, $E_o = 10^4$ V/m, $\epsilon_i = 4$, $\epsilon = 78.5$, $\kappa a = 30$, $z^+ = 1$, $z^- = -1$, $D^+ = D^- = 2\times10^{-9}$ m²/s, $\eta = 8.9\ 10^{-4}$ Pa s, $\rho_m = 10^3$ kg/m³, $T = 298.16$ K.

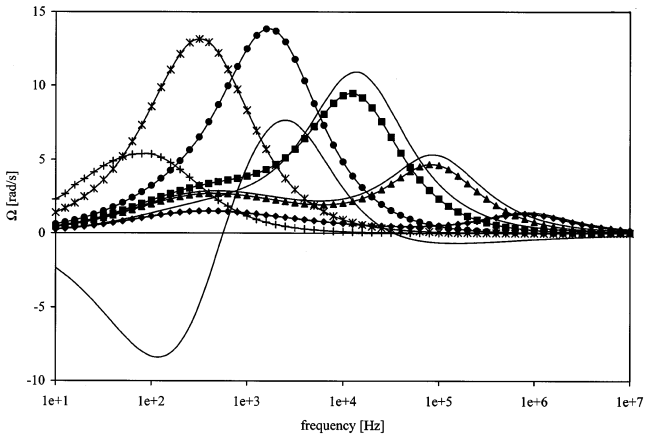

Figure 3. Same as Figure 2 for ζ = − 100 mV and different values of κa: (◆) 100, (▲) 30, (■) 10, (●) 3, (∗) 1, (+) 0.3. Theoretical curves for $\kappa a \leq 1$ are not shown (see text).

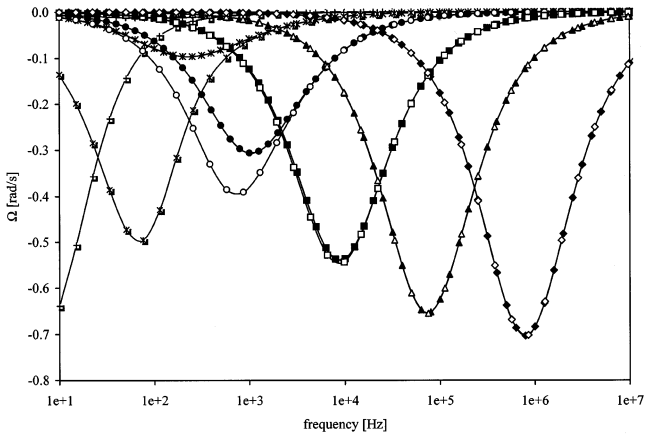

Figure 4. Electrorotation spectra obtained using numerical calculations (lines with solid symbols), analytical calculations with eq 27 (lines that exactly coincide with the numerical calculations), and full theoretical calculations (lines with empty symbols). Same data as in Figure 3, but for noncharged particles (ζ = 0).

The expression used for the numerical calculation of the electrorotation velocity (eq 27) has a general character, since it

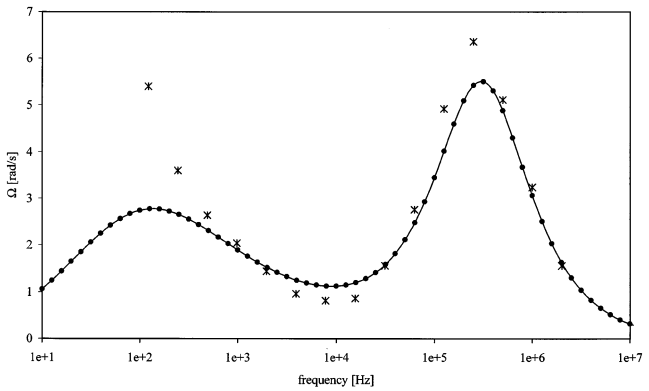

Figure 5. Experimental data for the electrorotation velocity obtained by Arnold et. al[6] (∗), compared with a numerical spectrum (●). The parameters used are: $a = 2.65\ \mu$m, $\zeta = -150$ mV, $E_o = 9580$ V/m, $\epsilon_i = 4$, $\epsilon = 78.5$, $\sigma = 7\ 10^{-4}$ S/m, $z^+ = 1$, $z^- = -4$, $D^+ = 2\times10^{-9}$ m^2/s, $D^- = 0.4\times10^{-9}$ m^2/s, $\eta = 9.78\times10^{-4}$ Pa s, $\rho_m = 10^3$ g/m^3, $T = 298.16$ K.

is not based on the thin double layer approximation. Nevertheless, it should not be combined with theoretical models for charged suspended particles, since the ion concentrations and potential distributions calculated in these models already include the thin double layer approximation. Therefore, the use of eq 27 would not improve the results obtained in preceding papers,[22,24] but would only complicate the calculations by the addition of a numerical integration.

A different situation arises for noncharged particles, since in this case it is possible to analytically obtain the exact solution for the ion concentrations and potential distributions, irrespective of the value of κa. Therefore, combining these results with eq 27 should lead to an exact solution of the electrorotation velocity. This can be seen in Figure 4, where the electrorotation spectra of noncharged particles obtained using eq 27 with analytical expressions for $\delta\phi(r)$ and $g(x)$ are compared with numerical results for different values of κa. Full theoretical results calculated as in previous works,[24] are also represented. No differences can be seen between the numerical results and the theoretical results calculated using eq 27. Moreover, for large values of κa, all three methods lead to the same results. However, as the value of κa is lowered, the spectra obtained using the previous theoretical method start to increasingly differ from the results of the other two calculations.

Finally, Figure 5 shows the experimental results obtained by Arnold et al.[6] together with a numerical spectrum. To simulate the electrolyte solution used in the experiments (a solution of ethylenediaminetetraacetic acid adjusted to pH 7 with KOH), the diffusion coefficients and valences of the positive and negative ions used in the calculation correspond to potassium and ethylenediaminetetraacetic ions, respectively. While a much better agreement is achieved than in reference 22, differences still persist in both the characteristic frequency and the amplitude of the low-frequency peak. They could possibly be due to the hypothesis, derived from the standard model, that the radius of the particle coincides with the slipping plane. The removal of this hypothesis was shown to improve the agreement between theory and experimental data obtained from electrophoretic and dielectric response measurements of some colloidal "nonideal" systems.[30,31] Another possible cause for this discrepancy could be ascribed to the fact that the electrolyte solution used in the experiment is made of a weak acid, so that it cannot be reproduced with the model used in this work, which assumes that the electrolyte is strong. While there are some theoretical[32] and numerical[33] works dealing with electrokinetic and dielectric properties of colloidal suspensions in weak electrolyte solutions, to our knowledge there is no general theory or numerical calculation for the response of weak electrolyte suspensions to AC electric fields.

In conclusion, the use of a numerical method in the solution of the problem presented in this work improves the results in many aspects. First, the induced dipole coefficient is solved without using the thin double-layer approximation. This is a prerequisite for the use of eq 27 in order to calculate the electrorotation velocity, avoiding the flat interface approximation previously used in the calculation of the electroosmotic contribution to rotation. Finally, it allows that different valences of positive and negative ions can be considered, and opens the possibility to extend the model to more complex particle and/or electrolyte solution models, which cannot be treated theoretically without using too many approximations. Indeed, the extension to cells with membrane and a charged cell wall is being currently developed.

Acknowledgment. This work was partially supported by grant 26/E220 of the Consejo de Investigaciones de la Universidad Nacional de Tucumán, project BFM2000-1099 of the Ministry of Science and Technology of Spain, and by FOMEC and FACEyT fellowships to V.Z.

Appendix

Generic compartments for each branch of the complete network are represented in Figure 6. The resistances (R), capacitors (C), voltage controlled current sources (G), voltage controlled voltage sources (E), and voltage sources (V) have the following values:

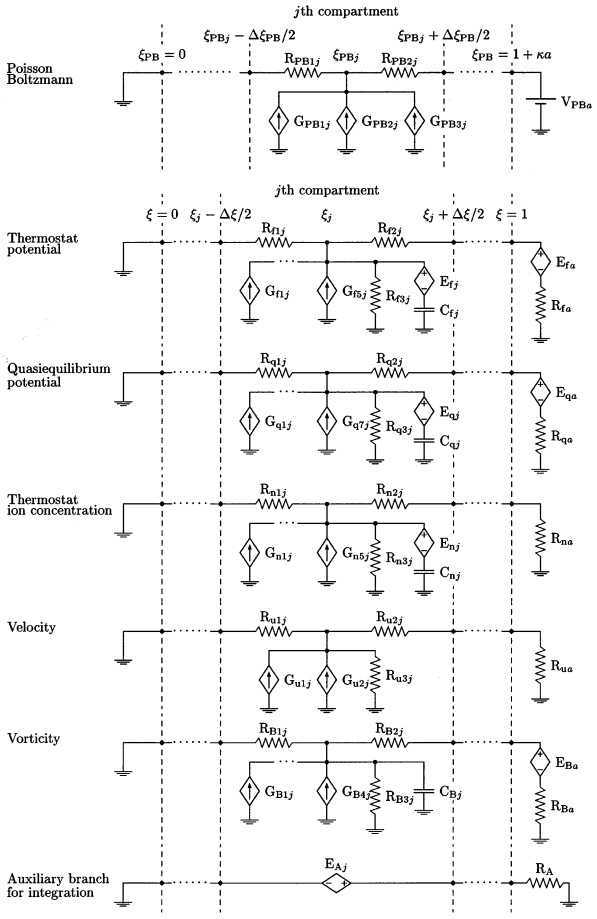

Figure 6. Schematic representation of the network used to solve the equation system.

$$R_1 = R_2 = \frac{\Delta\xi}{2}$$

$$R_{f3j} = \frac{\xi_j^2}{2\Delta\xi + (z^+ + z^-)\xi_j \Delta\tilde{\phi}_o(\xi_j)}$$

$$R_{q3j} = \left[\frac{2\Delta\xi}{\xi_j^2} + \frac{e^2a^2\Delta\xi}{\epsilon_o\epsilon kT\,\xi^4}((z^+)^2C_o^+(\xi_j) + (z^-)^2C_o^-(\xi_j))\right]^{-1}$$

$$R_{n3j} = R_{u3j} = R_{B3j} = \frac{\xi_j^2}{2\Delta\xi}$$

$$R_{fa} = R_{na} = 2R_{ua} = R_{Ba} = 1$$

$$R_{qa} = \frac{\epsilon_e}{\epsilon_i + \epsilon_e}$$

$$R_A = 10000$$

$$V_{PBa} = \tilde{\xi}$$

$$C_{fj} = \frac{C_{qj}}{Q} = C_{nj} = \frac{\eta}{\rho_m D_{ef}} C_{Bj} = \frac{a^2\,\Delta\xi}{D_{ef}\,\xi_j^4}$$

$$E_{fj} = f(\xi_j) + \Lambda\, n(\xi_j) + Q\, q(\xi_j)$$

$$E_{qj} = -\frac{\Lambda}{Q} n(\xi_j)$$

$$E_{nj} = z^+z^-\Lambda\, q(\xi_j)$$

$$E_{Aj} = \frac{kTa^2\Delta\tilde{\phi}_o(\xi_j)}{\eta D_{ef}\,\xi_j}\Bigg[((z^+)^2C_o^+(\xi_j) + (z^-)^2C_o^-(\xi_j))\left(\frac{eaE_o}{kT\xi_j^2} - f(\xi_j)\right) - (z^+C_o^+(\xi_j) + z^-C_o^-(\xi_j))n(\xi_j)\Bigg]$$

$$E_{fa} = -\frac{eaE_o}{kT}$$

$$E_{qa} = \frac{\epsilon_i}{\epsilon_i + \epsilon_e}\left(\frac{eaE_o}{kT} - f(\xi_j)\right)$$

$$E_{Ba} = V_A(\xi = 1)$$

$$G_{PB1j} = \frac{\kappa^2 r(\xi_{PBj})(r(\xi_{PBj})\,\xi_{PBj} - a)}{[\kappa a - \xi_{PBj}(1 + \kappa r(\xi_{PBj}))]^2}\Delta\tilde{\phi}_o(\xi_j)$$

$$G_{PB2j} = \frac{e^2\Delta\xi_{PB} r^2(\xi_{PBj})\, z^+c_\infty^+}{\epsilon_o\epsilon\, kT\,[\kappa a - \xi_{PBj}(1 + \kappa r(\xi_{PBj}))]^2}\exp[-z^+\,\tilde{\phi}_o(\xi_j)]$$

$$G_{PB3j} = \frac{e^2\Delta\xi_{PB} r^2(\xi_{PBj})\, z^-c_\infty^-}{\epsilon_o\epsilon\, kT\,[\kappa a - \xi_{PBj}(1 + \kappa r(\xi_{PBj}))]^2}\exp[-z^-\,\tilde{\phi}_o(\xi_j)]$$

$$G_{f1j} = -G_{q1j} = -\left(\frac{z^+ + z^-}{z^+z^-}\right)G_{n1j} = -(z^+ + z^-)\frac{eaE_o}{kT\,\xi_j^3}\Delta\tilde{\phi}o(\xi_j)$$

$$G_{f2j} = -G_{q2j} = -\frac{\Delta\tilde{\phi}_o(\xi_j)\,\Delta n(\xi_j)}{\Delta\xi}$$

$$G_{f3j} = \left[\frac{2}{\xi_j} - \frac{(z^+ + z^-)\Delta\tilde{\phi}_o(\xi_j)}{\Delta\xi}\right]\Delta f(\xi_j)$$

$$G_{f4j} = -\frac{\Delta\tilde{\phi}_o(\xi_j)\, n(\xi_j)}{\xi_j}$$

$$G_{f5j} = -G_{q7j} = \frac{Q}{z^+z^-\Lambda}G_{n5j} = \frac{Q\Delta\tilde{\phi}_o(\xi_j)}{\xi_j}\left[\frac{u(1)}{\xi_j^2} - u(\xi_j)\right]$$

$$G_{q3j} = \frac{2}{\xi_j}\Delta q(\xi_j)$$

$$G_{q4j} = \left(\frac{z^+ + z^-}{z^+z^-}\right)G_{n3j} = (z^+ + z^-)\,\frac{\Delta\tilde{\phi}_o(\xi_j)\,\Delta f(\xi_j)}{\Delta\xi}$$

$$G_{q5j} = \left(\frac{z^+ + z^-}{z^+z^-}\right)G_{n4j} = (z^+ + z^-)\,\frac{\Delta\tilde{\phi}_o(\xi_j)\, f(\xi_j)}{\xi_j}$$

$$G_{q6j} = \left[\frac{\Delta\tilde{\phi}_o(\xi_j)}{\xi_j} + \frac{e^2a^2\Delta\xi}{\epsilon_o\epsilon kT\,\xi^4}(z^+C_o^+(\xi_j) + z^-Co^-(\xi_j))\right]n(\xi_j)$$

$$G_{n2j} = \frac{2}{\xi_j}\Delta n(\xi_j)$$

$$G_{u1j} = \frac{2}{\xi_j}\Delta u(\xi_j)$$

$$G_{u2j} = \frac{2\Delta\xi}{\xi_j^5}B(\xi_j)$$

$$G_{B1j} = -\frac{ea^3E_o\Delta\tilde{\phi}_o(\xi_j)}{\eta D_{ef}\xi_j^2}((z^+)^2Co^+(\xi_j) + (z^-)^2Co^-(\xi_j))$$

$$G_{B2j} = \frac{a^2kT\Delta\tilde{\phi}_o(\xi_j)}{\eta D_{ef}}((z^+)^2C_o^+(\xi_j) + (z^-)^2Co^-(\xi_j))\, f(\xi_j)$$

$$G_{B3j} = \frac{a^2kT\Delta\tilde{\phi}_o(\xi_j)}{\eta D_{ef}}(z^+Co^+(\xi_j) + z^-Co^-(\xi_j))\, n(\xi_j)$$

where

$$\Delta\tilde{\phi}_o(\xi_j) = [\tilde{\phi}_o(\xi_{j+1/2}) - \tilde{\phi}_o(\xi_{j-1/2})]$$

$$\Delta f(\xi_j) = [f(\xi_{j+1/2}) - f(\xi_{j-1/2})]$$

$$\Delta q(\xi_j) = [q(\xi_{j+1/2}) - q(\xi_{j-1/2})]$$

$$\Delta n(\xi_j) = [n(\xi_{j+1/2}) - n(\xi_{j-1/2})]$$

References and Notes

(1) Dukhin, S. S.; Semenikhin, N. M. *Kolloidn. Zh.* **1970**, *32*, 366.
(2) Dukhin, S. S.; Shilov, V. N. *Dielectric phenomena and the double layer in disperse systems and polyelectrolyte*; Wiley: New York, 1974.
(3) Lyklema, J. *Fundamentals of Interface and Colloid Science, Vol. II Solid−Liquid Interfaces*; Academic Press: New York, 1995.
(4) Grosse, C.; Shilov, V. N. *J. Phys. Chem.* **1996**, *100*, 1771.
(5) Grosse, C.; Tirado, M.; Pieper, W.; Pottel, R. *J. Colloid Interface Sci.* **1998** *205*, 26.
(6) Arnold, W. M.; Schwan, H. P.; Zimmermann, U. *J. Phys. Chem.* **1987**, *91*(19), 5093.
(7) Gimsa, J.; Prüger, B.; Eppmann, P.; Donath, E. *Colloids Surf. A* **1995**, *98*, 243.
(8) Maier, H. *Biophys. J.* **1997**, *73*, 1617.

(9) Eppmann, P.; Prüger, B.; Gimsa, J. *Colloids Surf. A* **1999**, *149*, 443.
(10) Markx, G. H.; Pethig, R.; Rousselet, J. *J. Phys. D: Appl. Phys.* **1997**, *30*, 2470.
(11) DeLacey, E. H. B.; White, L. R. *J. Chem. Soc., Faraday Trans.* **1981**, *77*(2), 2007.
(12) López-García, J. J.; Horno, J.; González-Caballero, F.; Grosse, C.; Delgado, A. V. *J. Colloid Interface Sci.* **2000**, *228*, 95.
(13) O'Brien, R. W.; White, L. R. *J. Chem. Soc., Faraday Trans.* **1978**, *74*(2), 1607.
(14) Mangelsdorf, C. S.; White, L. R. *J. Chem. Soc., Faraday Trans.* **1992**, *88*(24), 3567.
(15) Sauer, F. A.; Schlögl, R. W. In *Interactions Between Electromagnetic Fields and Cells*; Chiabrera, A., Nicolini, C., Schwan, H. P., Eds.; Plenum: New York, 1985; pp 203−251.
(16) Fuhr, G.; Glaser, R.; Hagedorn, R. *Biophys. J.* **1986**, *49*, 395.
(17) Arnold, W. M.; Zimmermann, U. *J. Electrostatics* **1988**, *21*, 151.
(18) Kakutani, T.; Shibatani, S.; Sugai, M. *Bioelectrochem. Bioenerg.* **1993**, *31*, 131.
(19) Hughes, M. P.; Wang, X.-B.; Becker, F. F.; Gascoyne, P. R. C.; Pethig, R. *J. Phys. D: Appl. Phys.* **1994**, *27*, 1564.
(20) Holzel, R. *J. Phys. D: Appl. Phys.* **1993**, *26*, 2112.
(21) Goater, A. D.; Burt, J. P. H.; Pethig, R. *J. Phys. D: Appl. Phys.* **1997**, *30*, L65.
(22) Grosse, C.; Shilov, V. N. *Colloids Surf. A* **1998**, *140*, 199.
(23) Zimmerman, V.; Grosse, C.; Shilov, V. N. *Colloids Surf. A* **1999**, *159*, 299.
(24) Zimmerman, V.; Grosse, C. *Colloids Surf. A* **2002**, *197*, 69.
(25) López-García, J. J.; Horno, J.; Delgado, A. V.; González-Caballero, F. *J. Phys. Chem. B* **1999**, *103*, 11297.
(26) Shilov, V. N.; Delgado, A. V.; González-Caballero, F.; Horno, J.; López-García, J. J.; Grosse, C. *J. Colloid Interface Sci.* **2000**, *232*, 141.
(27) Horno, J.; González-Fernández, C. F.; Hayas, A.; González-Caballero, F. *Biophys. J.* **1989**, *55*, 527.
(28) O'Konski, C. T. *J. Phys. Chem.* **1960**, *64*, 605.
(29) Grosse, C.; Arroyo, F. J.; Shilov, V. N.; Delgado, A. V. *J. Colloid Interface Sci.* **2001**, *242*, 75.
(30) Rosen, L. A.; Baygents, J. C.; Saville, D. A. *J. Chem. Phys.* **1993**, *98*(5), 4183.
(31) Gittings, M. R.; Saville, D. A. *Langmuir* **1995**, *11*, 798.
(32) Grosse, C.; Shilov, V. N. *J. Colloid Interface Sci.* **2000**, *225*, 340.
(33) Baygents, J. C.; Saville, D. A. *J. Colloid Interface Sci.* **1991**, *146*(1), 9.